

RESEARCH ARTICLE

PLC ζ is the physiological trigger of the Ca²⁺ oscillations that induce embryogenesis in mammals but conception can occur in its absence

Alaa Hachem^{1,*}, Jonathan Godwin^{2,*}, Margarida Ruas^{1,*}, Hoi Chang Lee³, Minerva Ferrer Buitrago⁴, Goli Ardestani³, Andrew Bassett⁵, Sebastian Fox¹, Felipe Navarrete³, Petra de Sutter⁴, Björn Heindryckx⁴, Rafael Fissore³ and John Parrington^{1,†}

ABSTRACT

Activation of the egg by the sperm is the first, vital stage of embryogenesis. The sperm protein PLC ζ has been proposed as the physiological agent that triggers the Ca²⁺ oscillations that normally initiate embryogenesis. Consistent with this, recombinant PLC ζ induces Ca²⁺ oscillations in eggs and debilitating mutations in the *PLCZ1* gene are associated with infertility in men. However, there has been no evidence that knockout of the gene encoding PLC ζ abolishes the ability of sperm to induce Ca²⁺ oscillations in eggs. Here, we show that sperm derived from *Plcz1*^{-/-} male mice fail to trigger Ca²⁺ oscillations in eggs, cause polyspermy and thus demonstrate that PLC ζ is the physiological trigger of these Ca²⁺ oscillations. Remarkably, some eggs fertilized by PLC ζ -null sperm can develop, albeit at greatly reduced efficiency, and after a significant time-delay. In addition, *Plcz1*^{-/-} males are subfertile but not sterile, suggesting that in the absence of PLC ζ , spontaneous egg activation can eventually occur via an alternative route. This is the first demonstration that *in vivo* fertilization without the normal physiological trigger of egg activation can result in offspring. PLC ζ -null sperm now make it possible to resolve long-standing questions in fertilization biology, and to test the efficacy and safety of procedures used to treat human infertility.

KEY WORDS: Sperm, Egg, Embryogenesis, Calcium signalling, PLC ζ , Mouse

INTRODUCTION

Infertility is a world health problem that affects an estimated 1 in 7 couples and can be caused by problems in the development of viable gametes, but also by defects in fertilization or embryo development. Activation of the egg by the sperm at fertilization is a fundamental event in embryogenesis, and has been of scientific interest since Jacques Loeb's pioneering studies in the 1890s (Parrington et al., 2007). Defects in this process underlie some cases of human male infertility (Escoffier et al., 2016; Heytens et al., 2009; Kashir et al., 2012), and may have relevance for more general problems of embryo

development in humans. In mammals, egg activation is triggered by sperm-induced Ca²⁺ oscillations in the egg (Igusa and Miyazaki, 1986; Kline and Kline, 1992). A key role of these Ca²⁺ oscillations is to downregulate, via a signalling pathway involving the Ca²⁺-dependent protein kinase gamma (CamKII γ) and early mitotic inhibitor (Emi2), the maturation promotion factor (MPF) responsible for the metaphase II arrest of the egg (Sanders and Swann, 2016; Sobinoff et al., 2013). A later decline in mitogen-activated protein kinase (MAPK) activity correlates with the formation of pronuclei and entry into interphase of the first cell cycle. Another important event triggered following sperm-egg fusion is the block of polyspermy, which involves both changes in the egg membrane linked to the shedding of the egg protein Juno (Bianchi et al., 2014), and the cortical reaction: the Ca²⁺-dependent exocytosis of cortical granules and hardening of the zona pellucida of the egg (Li et al., 2013).

Despite advances in our understanding of the signalling pathways that lie downstream of the sperm-induced Ca²⁺ oscillations, exactly how the sperm triggers such Ca²⁺ oscillations in the egg has remained controversial. Previous studies have provided evidence that the physiological trigger of the Ca²⁺ oscillations is a sperm protein called phospholipase C zeta (PLC ζ) (Ito et al., 2011; Swann and Lai, 2016). Thus, recombinant PLC ζ RNA or protein trigger Ca²⁺ oscillations when injected into eggs, and depletion of PLC ζ from sperm extracts eliminates their ability to trigger such Ca²⁺ oscillations (Kashir et al., 2011; Sanusi et al., 2015; Saunders et al., 2002). In addition, partial knockdown of *Plcz1* expression in mouse sperm using RNA interference leads to sperm-induced Ca²⁺ oscillations that terminate prematurely, to lower rates of egg activation and to no transgenic offspring after fertilization *in vivo* (Knott et al., 2005). Further evidence for an important physiological role for PLC ζ has come from the discovery of debilitating mutations in the *PLCZ1* gene that are associated with infertility in men (Escoffier et al., 2016; Heytens et al., 2009; Kashir et al., 2012). However, despite these pieces of evidence implicating PLC ζ as the physiological agent of egg activation, irrefutable evidence using genetic disruption methods to show that PLC ζ is the sole initiator of Ca²⁺ oscillations in mammalian eggs has been lacking, and recently doubts have been raised about a role for PLC ζ in the process of egg activation (Aarabi et al., 2012; Ferrer-Vaquer et al., 2016).

Another controversial issue is the importance of the Ca²⁺ oscillations induced by the sperm during mammalian fertilization for optimum embryo development. Although such oscillations constitute the physiological stimulus, previous studies have shown that egg activation and development to blastocyst *in vitro* can be induced by pharmacological or genetic treatments that reduce MPF levels in ways that do not require a Ca²⁺ stimulus (Knott et al., 2006; Miao et al., 2012; Phillips et al., 2002; Suzuki et al., 2010). In

¹Department of Pharmacology, University of Oxford, Mansfield Road, Oxford OX1 3QT, UK. ²Department of Biochemistry, University of Oxford, South Parks Road, Oxford OX1 3QU, UK. ³Department of Veterinary and Animal Sciences, University of Massachusetts, 661 North Pleasant Street, Amherst, MA 01003-9286, USA.

⁴Department for Reproductive Medicine, Ghent University Hospital, De Pintelaan 185, 9000 Ghent, Belgium. ⁵Sir William Dunn School of Pathology, University of Oxford, South Parks Road, Oxford OX1 3RE, UK.

*These authors contributed equally to this work

†Author for correspondence (john.parrington@pharm.ox.ac.uk)

DOI: 10.1242/dev.150227

addition, currently infertility in men whose sperm fail to induce egg activation can be successfully treated by mechanical, electrical or chemical stimuli that induce a Ca^{2+} signal that is far from physiological (Sfontouris et al., 2015; Vanden Meerschaut et al., 2014). Such approaches have led to the successful births of hundreds of human infants worldwide. However, other studies of mouse parthenogenetic embryos stimulated by different patterns of artificially induced Ca^{2+} transients (Ducibella et al., 2002), or fertilized mouse eggs whose endogenous Ca^{2+} oscillations have been inhibited or hyper-stimulated (Ozil et al., 2005), show that altering the number and frequency of Ca^{2+} transients can subtly affect embryonic gene expression and developmental potential. Therefore, the long-term safety implications of the use of artificial egg activation stimuli in clinical practice remain far from clear.

To address these issues further experimentally, what has been lacking is a mouse in which PLC ζ expression has been eliminated through gene knockout. This would make it possible to assess the physiological significance of PLC ζ . In addition, if sperm lacking expression of functional PLC ζ were found to be incapable of triggering Ca^{2+} oscillations in the egg, this would provide a null background in which to test the effects of artificial egg activation stimuli as inducers of egg activation and embryo development. Here, we describe the generation of such a PLC ζ -null mouse through CRISPR/Cas9 gene editing (Doudna and Charpentier, 2014), and its phenotypic analysis.

RESULTS

Generation of PLC ζ knockout mice using CRISPR/Cas9 gene editing

To create a PLC ζ -null mouse, we used CRISPR/Cas9 gene editing to target the *Plcz1* gene in fertilized mouse eggs. Two strategies were employed that targeted different exons of *Plcz1* with independent single guide RNAs (sgRNAs) to control for potential off-target mutagenesis: one used Cas9^{WT} endonuclease with one sgRNA; the other used Cas9^{D10A} nickase with two paired sgRNAs (Fig. 1A). This second strategy was employed because it reduces off-target mutations (Ran et al., 2013; Shen et al., 2014). Two mutant *Plcz1* mouse lines were produced, originating from two F0 females harbouring frameshift-producing deletions: *Plcz1*^{em1Jparr}, generated using Cas9^{D10A} nickase, has a 22-nucleotide deletion in exon 3 (Fig. 1B,D); *Plcz1*^{em2Jparr}, generated using Cas9^{WT} endonuclease, has a 17-nucleotide deletion in exon 5 (Fig. 1C,D).

Sequence analysis of RT-PCR products from testis mRNA obtained from these two lines confirmed that these corresponded to the predicted mutant cDNA sequences with no observable residual wild-type *Plcz1* (*Plcz1*^{WT}) sequence contamination (Fig. 2A,C), suggesting complete lack of *Plcz1*^{WT} expression in these mutant lines. The truncated proteins that could be produced from the two mutant *Plcz1* alleles (Fig. 2B,D) correspond to small N-terminal sequences lacking regions necessary for enzymatic activity (Nomikos et al., 2013). The absence of full-length PLC ζ was further confirmed by immunoblotting analysis of sperm derived from *Plcz1*^{em1Jparr} mice (Fig. 2E).

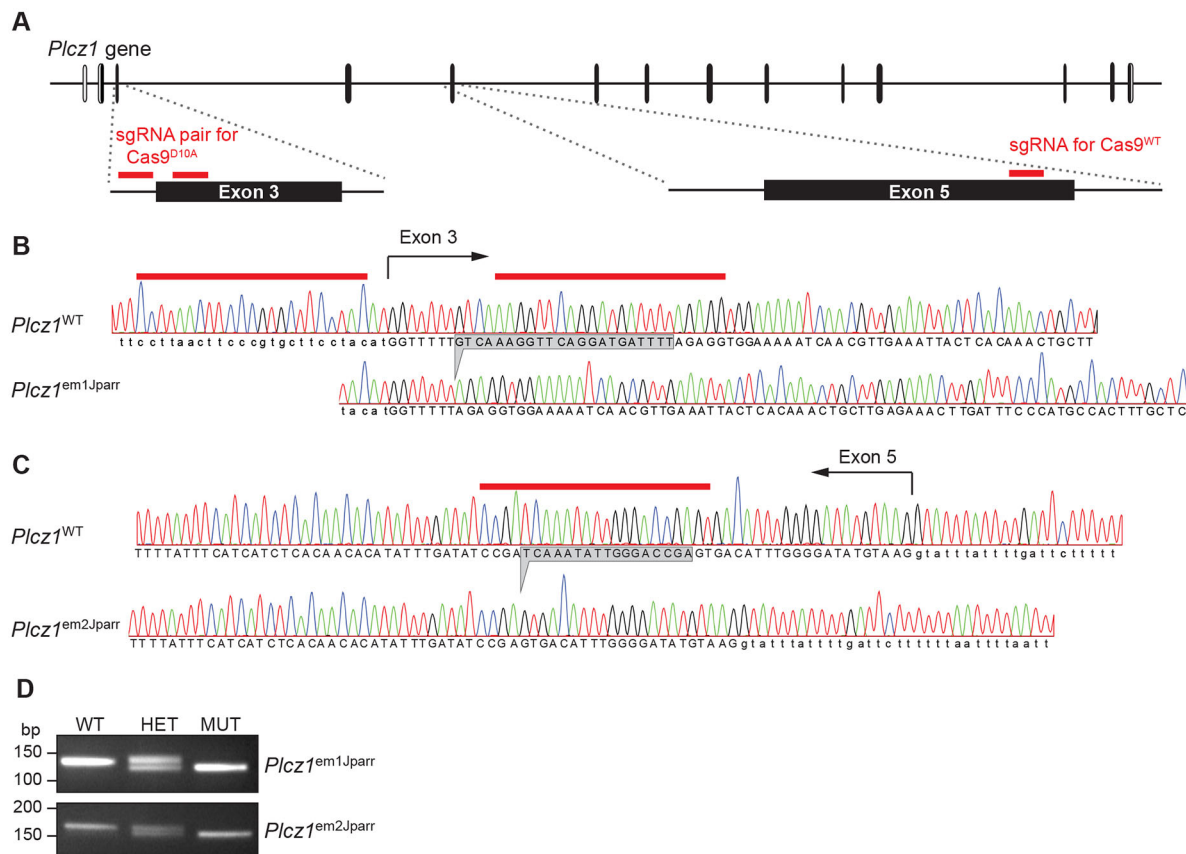


Fig. 1. Genomic characteristics of mouse *Plcz1*^{em1Jparr} and *Plcz1*^{em2Jparr} mutant alleles. (A) Gene structure of the mouse *Plcz1* gene (NM_054066.4) and target sequences (red lines) for CRISPR/Cas9. Exons are represented by vertical bars (unfilled, untranslated regions; filled, coding regions). (B,C) Comparison of genomic sequences from wild-type *Plcz1* (*Plcz1*^{WT}) allele and two mutant *Plcz1* alleles harbouring nucleotide deletions (deleted sequence shaded grey in *Plcz1*^{WT} sequence). Capital letters correspond to exonic sequences and lower case letters to intronic sequences. (D) Typical result from a genotyping PCR reaction for both *Plcz1* mutant lines: HET, *Plcz1*^{+/em1Jparr} or *Plcz1*^{+/em2Jparr}; MUT, homozygote *Plcz1*^{em1Jparr} or *Plcz1*^{em2Jparr}; WT, homozygote *Plcz1*^{WT}.

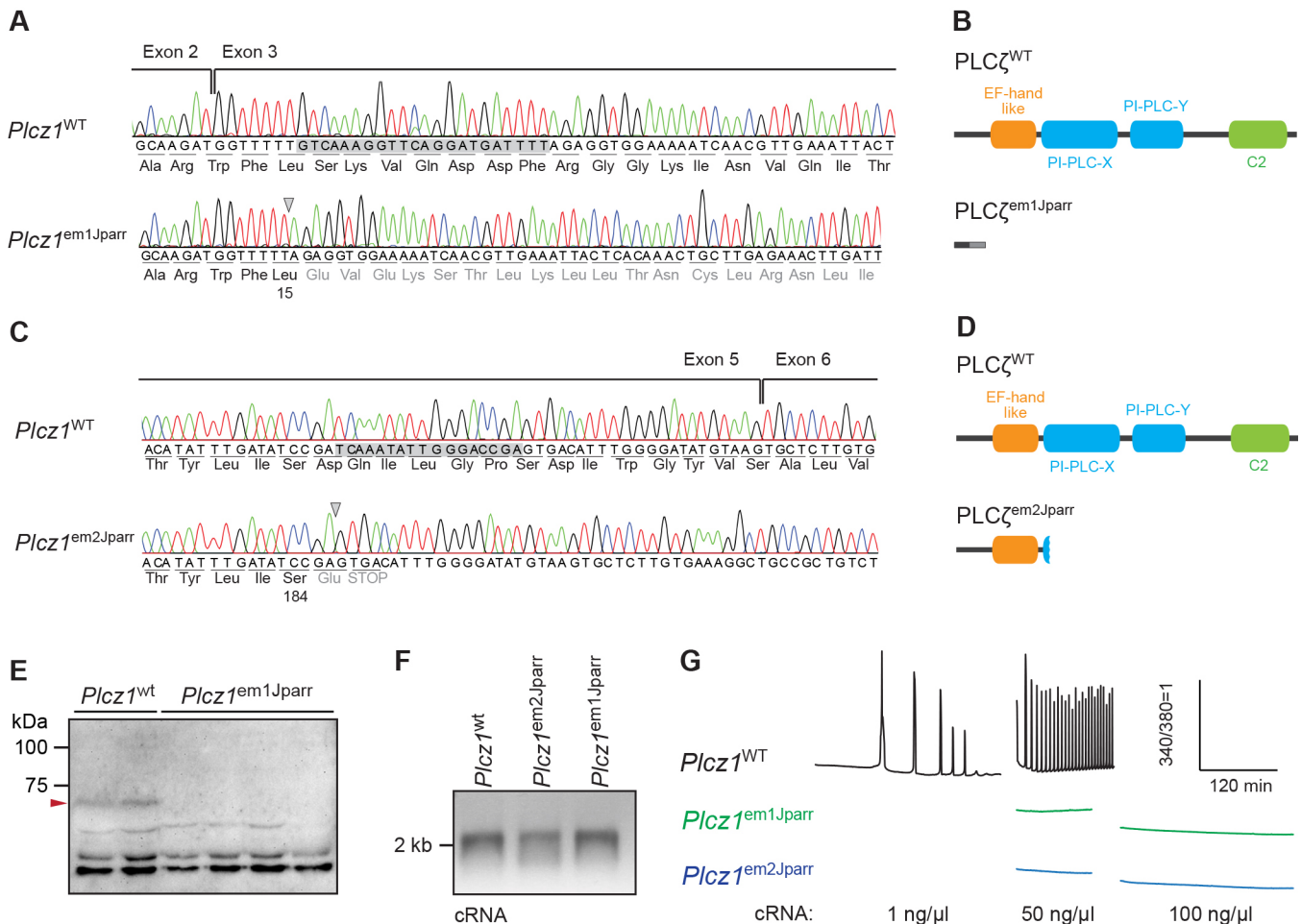


Fig. 2. Expression analysis of mouse *Plcz1*^{em1Jparr} and *Plcz1*^{em2Jparr} mutant alleles. (A,C) Comparison of cDNA sequences obtained from RT-PCR reactions using testis RNA from *Plcz1*^{WT} and homozygote *Plcz1*^{em1Jparr} (A) or *Plcz1*^{em2Jparr} (C) animals. Codons are underlined, with amino acids indicated by their three-letter code. Numbers below amino acids correspond to the last amino acid position within the primary sequence not affected by the frameshift. The amino acid sequence after the frameshift is in grey. (B,D) Predicted protein-domain structures for wild-type mouse PLCζ protein (PLCζ^{WT}) and truncated proteins resulting from expression of mutant PLCζ^{em1Jparr} (B) and PLCζ^{em2Jparr} (D) alleles. (E) Immunoblotting analysis of PLCζ in sperm from *Plcz1*^{WT} (two animals) and PLCζ^{em1Jparr} (four animals) using a custom-made anti-PLCζ antibody (Kurokawa et al., 2005). The immunoreactive band corresponding to PLCζ is indicated by a red arrow. (F) Agarose gel image showing integrity of *in vitro*-produced cRNA. (G) Typical Ca²⁺ responses, monitored by the fluorescence ratio of Fura-2 in wild-type mouse eggs, elicited by injection of recombinant copy RNA (cRNA) *in vitro* transcribed from *Plcz1*^{WT}, *Plcz1*^{em1Jparr} or *Plcz1*^{em2Jparr} cDNAs. Proportion of eggs showing Ca²⁺ oscillations: *Plcz1*^{WT} ([cRNA] 1 ng/μl=10/10; [cRNA] 50 ng/μl=8/8), *Plcz1*^{em1Jparr} ([cRNA] 50 ng/μl=5/5; [cRNA] 100 ng/μl=5/5) and *Plcz1*^{em2Jparr} ([cRNA] 50 ng/μl=5/5; [cRNA] 100 ng/μl=5/5).

It has been previously suggested that the post-acrosomal WW domain-binding protein (*Wbp2nl*/PAWP), could function as the physiological agent of egg activation (Aarabi et al., 2014). We therefore investigated the status of *Wbp2nl*/PAWP expression in our *Plcz1* mutant lines. RT-qPCR analysis for *Wbp2nl* mRNA revealed that the *Plcz1* mutations present in our two *Plcz1* mutant lines have no detrimental effects upon *Wbp2nl* mRNA expression in testis (Fig. S1A). Furthermore, immunoblotting analysis for PAWP revealed no apparent differences in the level of PAWP protein between *Plcz1*^{WT}- and *Plcz1*^{em1Jparr}-derived sperm (Fig. S1B).

We next carried out functional analysis of the mutant *Plcz* RNA predicted to be expressed in the two mutant mouse lines. *Plcz1*^{WT} recombinant copy RNA (cRNA) (Fig. 2F) injected into mouse eggs triggered Ca²⁺ oscillations in a dose-dependent manner, consistent with production of functional PLCζ protein (Saunders et al., 2002) (Fig. 2G); however, injection of either mutant cRNA failed to

induce Ca²⁺ oscillations (Fig. 2G). In combination, these results indicate that these mutant *Plcz1* lines are null for functional PLCζ expression and will be referred to as *Plcz1*^{-/-}.

PLCζ knockout does not affect spermatogenesis or sperm quality parameters

Histological analysis of *Plcz1*^{-/-} male testes indicated no defects in spermatogenesis (Fig. 3A). Furthermore, epididymal sperm from *Plcz1*^{-/-} males (*Plcz1*⁻ sperm) had normal viability (Fig. 3B,C), motility (Fig. 3D) and hyperactivity, which reflect their ability to undergo capacitation (Fig. 3E-G). Additionally, the ability of *Plcz1*⁻ sperm to undergo the acrosome reaction in response to either progesterone or ionomycin was undistinguishable from the sperm of wild-type animals (*Plcz1*⁺ sperm) (Fig. 3H). Collectively, these results indicate that loss of PLCζ has no apparent detrimental effects upon spermatogenesis or parameters associated with the ability of the sperm to bind and fuse with the egg.

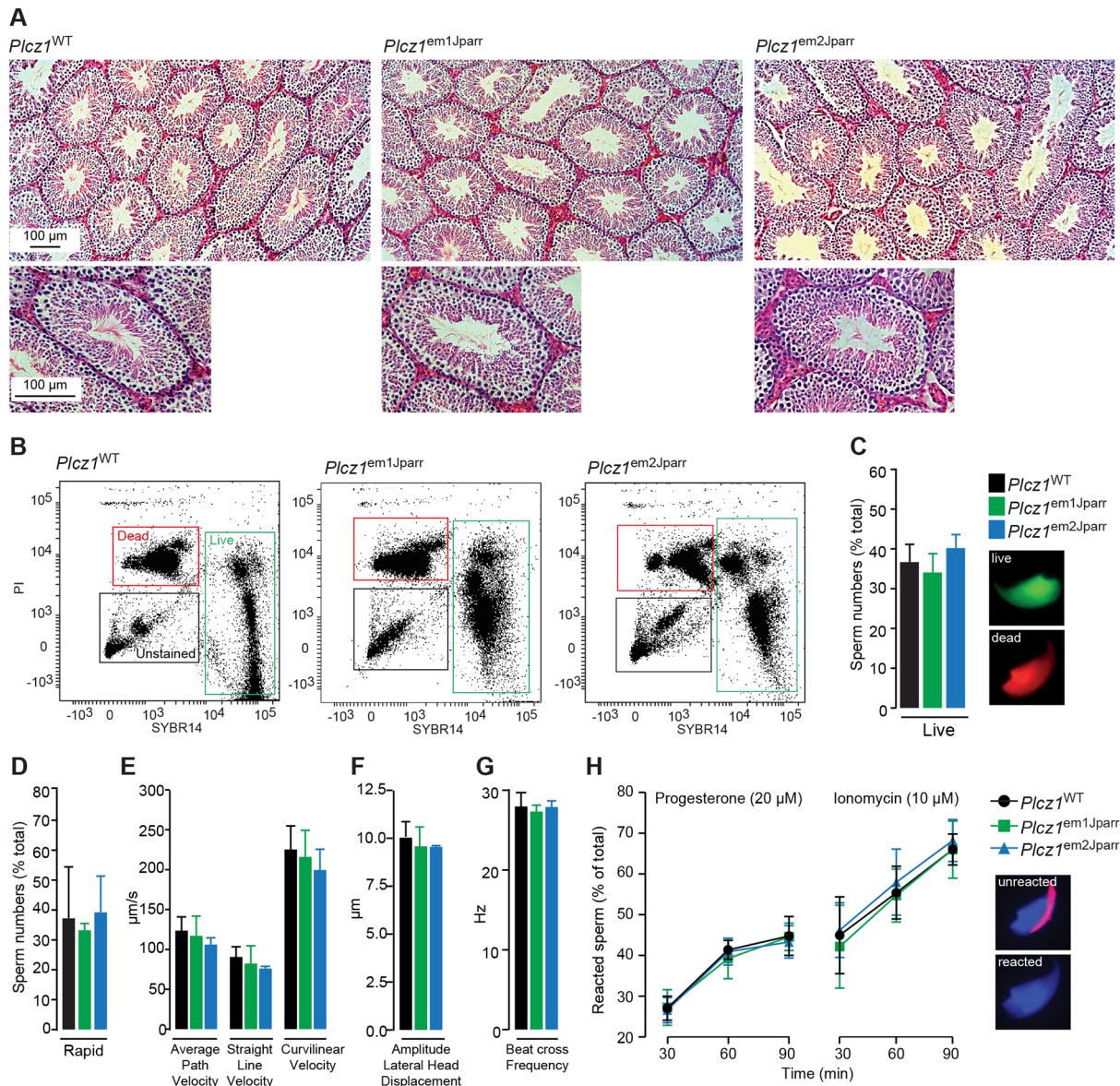


Fig. 3. Characterization of sperm from homozygote *Plcz1^{em1Jparr}* and *Plcz1^{em2Jparr}* mice. (A) Histological analysis of testes sections stained with Hematoxylin/Eosin. (B) Density plots of sperm stained with SYBR14 (live sperm) and propidium iodide (PI; dead sperm) and analysed by flow cytometry. A total of 10,000 events were collected for each group. (C) Quantification of data from B. Representative stained sperm were obtained using an Olympus BX40 microscope. (D-G) Analysis of sperm motility parameters using computer-assisted sperm analysis (CASA). (H) An acrosome reaction was induced either by treatment with progesterone or ionomycin, and reacted sperm were assessed by lack of reactivity towards fluorescently labelled lectin PNA. Representative images of reacted and unreacted sperm are shown. All data are presented as average \pm s.e.m. of four different animals. There are no statistically significant differences.

Loss of PLC ζ abolishes the ability of the sperm to trigger Ca²⁺ oscillations in the egg

Using intracytoplasmic sperm injection (ICSI), we next investigated whether *Plcz1^{-/-}* sperm could trigger Ca²⁺ oscillations in wild-type eggs. Injection of *Plcz1^{-/-}* sperm induced Ca²⁺ oscillations symptomatic of those seen at fertilization in nearly all eggs (Fig. 4A,B) (Wakai et al., 2011). In contrast, injected sperm from either *Plcz1^{-/-}* line failed to induce Ca²⁺ oscillations (Fig. 4A,B), which were nevertheless triggered by subsequent injection of *Plcz1^{WT}* cRNA (Fig. 4C). The inability of *Plcz1^{-/-}* sperm to trigger Ca²⁺ oscillations was further confirmed following *in vitro* fertilization (IVF) using zona pellucida-free eggs (Fig. 4D,E); while 16/34 eggs showed Ca²⁺ oscillations following IVF with *Plcz1^{WT}* sperm, none of the 40 eggs subjected to IVF with *Plcz1^{em1Jparr}*-derived sperm

showed such oscillations, with one egg showing a single Ca²⁺ transient (Fig. 4D,E). This is therefore the first direct evidence that PLC ζ is the sole physiological trigger of the Ca²⁺ oscillations responsible for egg activation in mammals (Wakai et al., 2011).

Increased polyspermy in eggs fertilized by PLC ζ -null sperm after IVF or *in vivo* fertilization

The inability of *Plcz1^{-/-}* sperm to trigger Ca²⁺ oscillations following IVF could be due to failure of *Plcz1^{-/-}* sperm to bind and fuse with the egg. However, no significant differences were observed in the percentage of eggs containing sperm heads after 6 h post-IVF with *Plcz1^{WT}*- or *Plcz1^{em1Jparr}*-derived sperm (*Plcz1^{WT}*, 143/193; *Plcz1^{em1Jparr}*, 103/132) assessed by Hoechst DNA staining (Fig. 5A). Remarkably, we noticed a dramatic increase in the rate

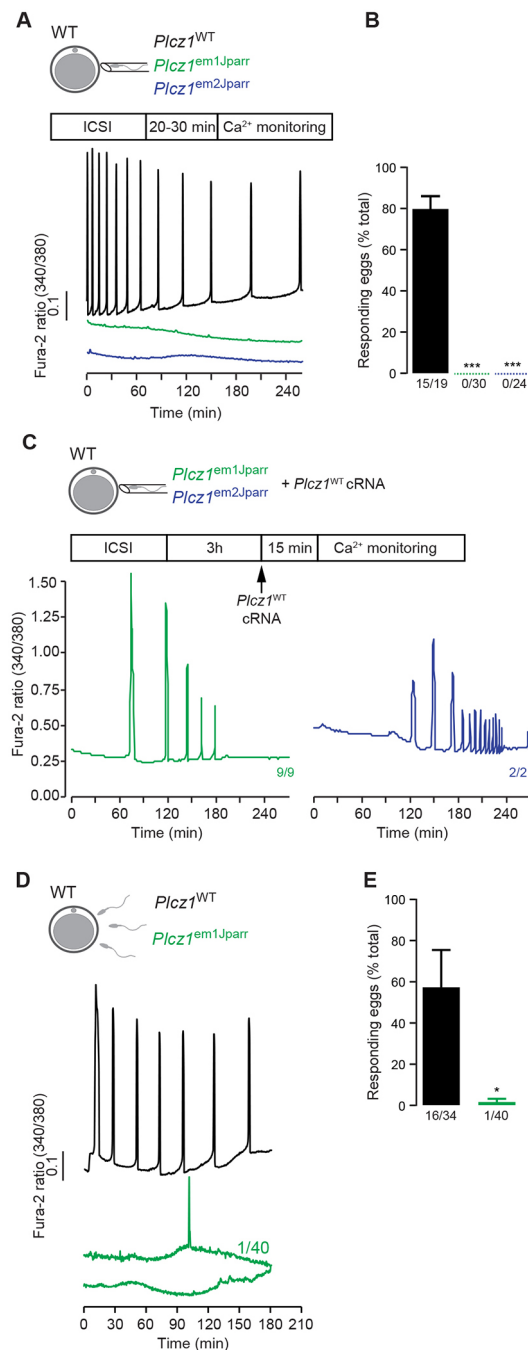


Fig. 4. Ca²⁺ responses elicited during fertilization of mouse eggs.

(A) Representative traces of Ca²⁺ responses, monitored by the fluorescence ratio (excitation 340/380 nm) of Fura-2, in wild-type mouse eggs, elicited by ICSI with sperm from homozygote *Plcz1*^{WT}, *Plcz1*^{em1Jparr} or *Plcz1*^{em2Jparr} males. (B) Compilation of results from all eggs subjected to ICSI. Data are presented as average ± s.e.m. followed by a one-way ANOVA analysis; numbers shown underneath each bar indicate proportion of responding eggs; the following number of animals were used for each group in a total of four or five experiments: *Plcz1*^{WT} (3), *Plcz1*^{em1Jparr} (2) and *Plcz1*^{em2Jparr} (4). (C) Representative traces of Ca²⁺ responses, monitored by the fluorescence ratio (excitation 340/380 nm) of Fura-2, in wild-type mouse eggs, elicited by injection of *Plcz1*^{WT} cRNA after ICSI with sperm from homozygote *Plcz1*^{em1Jparr} and *Plcz1*^{em2Jparr} males. Numbers shown next to traces indicate proportion of responding eggs subjected to ICSI and cRNA injection. (D) Representative traces of Ca²⁺ responses, in wild-type mouse eggs, elicited by IVF with sperm from *Plcz1*^{WT} and *Plcz1*^{em1Jparr} males; the *Plcz1*^{WT} control sperm were from a transgenic line of the same strain background as the *Plcz1*^{em1Jparr} sperm, in which the catalytic subunit of PKA was exclusively modified in the sperm (Morgan et al., 2008). (E) Compilation of results from all eggs subjected to IVF. Data are presented as average ± s.e.m. followed by Student's *t*-test; numbers shown underneath each bar indicate proportion of responding eggs; the following number of animals were used for each group in a total of four or five experiments: *Plcz1*^{WT} (5) and *Plcz1*^{em1Jparr} (1).

this failure is limited to cortical granule release is unknown; additional studies using *Plcz1*[−] sperm will be required to elucidate the status of other mechanisms that control the block to polyspermy and the role of Juno (Bianchi et al., 2014).

In vitro development of eggs fertilized by PLCζ-null sperm

As Ca²⁺ oscillations are considered to be the physiological trigger of mammalian egg activation (Fig. S2A,C) (Wakai et al., 2011), we assessed the ability of *Plcz1*[−] sperm to trigger this process. Following ICSI using *Plcz1*⁺ sperm, 35/40 of zygotes reached two-cell stage and 27/40 developed to the blastocyst stage (Fig. 6A). In contrast, *Plcz1*[−] sperm largely failed to trigger activation, with only a few eggs reaching the two-cell stage (*Plcz1*^{em1Jparr}, 2/36; *Plcz1*^{em2Jparr}, 1/47) and only one reaching the blastocyst stage (*Plcz1*^{em1Jparr}, 1/36; *Plcz1*^{em2Jparr}, 0/47) (Fig. 6A). This inability of *Plcz1*[−] sperm to trigger consistent egg activation was rescued by injection of *Plcz1*^{WT} cRNA 3 h after ICSI with a significant proportion of eggs now developing to the two-cell stage (*Plcz1*^{em1Jparr}, 16/20; *Plcz1*^{em2Jparr}, 6/9) (Fig. 6A).

The unexpected, albeit greatly reduced, ability of some eggs injected with sperm from *Plcz1*[−] males to undergo egg activation and development after ICSI could be caused by the injection protocol. To bypass this possible artefact, and others associated with *in vitro* fertilization procedures, we directly examined fertilization and embryo development of wild-type eggs from females fertilized *in vivo* by *Plcz1*^{+/+} and *Plcz1*^{−/−} males. Eggs/zygotes were collected at 18 h post-hCG and allowed to develop *in vitro* during which time they were routinely examined. At the early time point of 18 h, differences in activation events were already obvious, as *Plcz1*⁺ fertilized eggs displayed pronuclei formation, whereas *Plcz1*[−] fertilized eggs showed mostly condensed sperm head(s) (Fig. 6B). Thus, *Plcz1*[−] sperm induced egg activation much less efficiently and protractedly, as further observed at subsequent time points (Fig. 6C): eggs fertilized by *Plcz1*⁺ sperm showed a high rate of two pronuclei formation (19/25) by 22 h and cleavage to two cells (18/25) by 32 h post-hCG treatment, whereas eggs fertilized by *Plcz1*[−] sperm displayed only two pronuclei formation (*Plcz1*^{em1Jparr}, 6/120; *Plcz1*^{em2Jparr}, 1/43) by 25 h and cleavage to the two-cell stage (*Plcz1*^{em1Jparr}, 23/120; *Plcz1*^{em2Jparr}, 9/43) after 38 h post-hCG treatment (Fig. 6C).

of polyspermy among eggs fertilized by IVF with *Plcz1*[−] sperm when compared with *Plcz1*⁺ sperm (*Plcz1*^{WT}, 24/143; *Plcz1*^{em1Jparr}, 74/103) (Fig. 5B).

To discount possible artefacts associated with IVF, we investigated the levels of polyspermy in wild-type eggs from females fertilized *in vivo* by *Plcz1*^{+/+} and *Plcz1*^{−/−} males. Hoechst DNA staining at 18 h post-hCG showed a clear increase in polyspermy among eggs fertilized by *Plcz1*^{−/−} males (*Plcz1*^{em1Jparr}, 21/111; *Plcz1*^{em2Jparr}, 19/82) versus eggs fertilized by *Plcz1*^{+/+} males (3/37) (Fig. 5C), which confirms the findings observed following IVF.

These results indicate therefore that *Plcz1*[−] sperm are normal, regarding their ability to penetrate the egg, but suggest that, in the absence of Ca²⁺ oscillations, the mechanisms that block polyspermy (Fig. S2A,B) are not engaged in a timely fashion. Whether or not

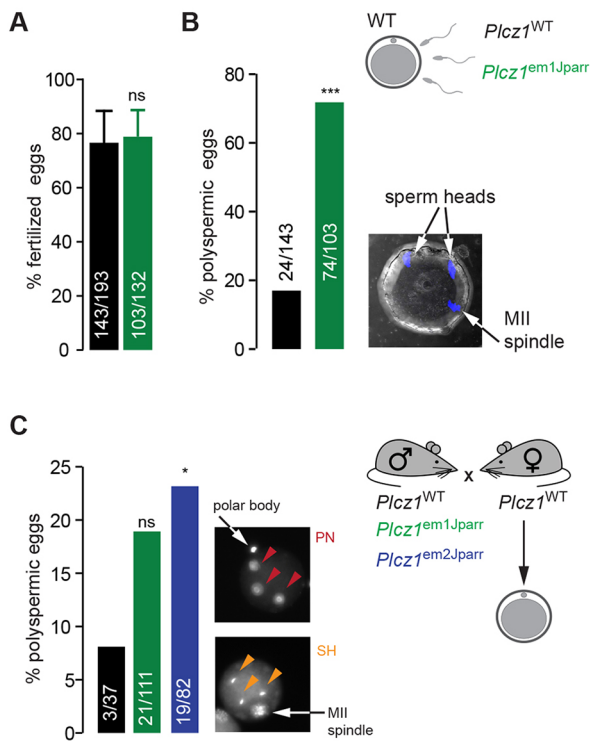


Fig. 5. Increased polyspermy in eggs fertilized by *Plcz1*^{em1Jparr} and *Plcz1*^{em2Jparr} mutant sperm. (A,B) Wild-type eggs were stained with Hoechst 6 h post-IVF with *Plcz1*^{WT}- and *Plcz1*^{em1Jparr}-derived sperm (*Plcz1*^{WT}: 193 eggs, 1 male; *Plcz1*^{em1Jparr}: 132 eggs, 1 male). (A) Percentage of eggs showing sperm penetration as indicative of fertilization. (B) Percentage of eggs showing abnormal number (>1) of sperm heads. Data are presented as percentage of total eggs examined from three combined experiments. An example of a fertilized egg showing polyspermy is shown. (C) Number of polyspermic eggs derived from super-ovulated wild-type females fertilized *in vivo* by homozygote *Plcz1*^{WT}, *Plcz1*^{em1Jparr} or *Plcz1*^{em2Jparr} males. Eggs were stained with Hoechst 18 h post-hCG treatment of females, for visualization of abnormal number of pronuclei (>2 PN) or sperm heads (>1 SH). Data are presented as percentage of total eggs examined from combined experiments (*Plcz1*^{WT}, 37 eggs, 2 male; *Plcz1*^{em1Jparr}, 111 eggs, 3 males; *Plcz1*^{em2Jparr}, 82 eggs, 2 males) and statistical analysis performed using a 2×2 contingency table followed by a Fisher's exact test. Examples of fertilized eggs showing polyspermy are shown.

PLCζ knockout male mice are subfertile

We next examined how the inability of *Plcz1*⁻ sperm to trigger Ca²⁺ oscillations could affect the capacity of *Plcz1*⁻ males to produce live offspring. Table 1 shows the compilation of results from various crosses. We found that, unlike crosses between *Plcz1*^{+/-} males and females or between *Plcz1*^{-/-} females and *Plcz1*^{+/-} males, which resulted in offspring similar in number to *Plcz1*^{+/+} crosses and with genotypes close to Mendelian proportions, *Plcz1*^{-/-} males could produce offspring, but at a much reduced efficiency compared with *Plcz1*^{+/+} males. Thus, although wild-type females crossed with *Plcz1*^{+/-} males produced average litter sizes of 7.8±0.8 and an average of 12.7±1.8 pups per female over the initial mating period of 10 weeks, wild-type females crossed with homozygote *Plcz1*^{em1Jparr} or *Plcz1*^{em2Jparr} males produced smaller litter sizes (4.2±0.6 or 3.2±1.2, respectively) with an average of 4.9±1.2 and 2.3±1.0 pups per female, respectively, over the same time period. This is the first demonstration in mammals that natural mating resulting *in vivo* fertilization without the normal physiological trigger of egg activation can result in offspring.

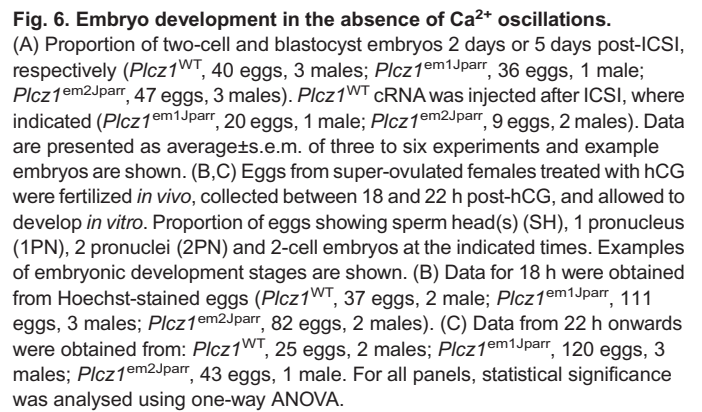
DISCUSSION

In summary, our findings demonstrate that absence of functional PLCζ does not compromise spermatogenesis and sperm quality parameters such as viability, motility, hyperactivity and ability to undergo the acrosome reaction. This is in contrast to a previous preliminary report that claimed that *Plcz1*^{-/-} male mice were defective in the spermatogenic process (Ito et al., 2011). However, we show that *Plcz1*⁻ sperm lack the ability to induce Ca²⁺ oscillations in the egg. Thus, we provide the first direct evidence that PLCζ is the physiological trigger of Ca²⁺ oscillations in mouse eggs, and probably in eggs of all mammals. Remarkably, a few eggs fertilized by *Plcz1*⁻ sperm can develop to the blastocyst stage *in vitro*, and natural mating of *Plcz1*^{-/-} males with wild-type females also results in low rates of egg activation that nevertheless can lead to development to term. Importantly, this is the first demonstration in mammals that natural mating and fertilization without the normal physiological trigger of egg activation can result in offspring. These findings are significant because PLCζ-null sperm and embryos offer a way to test the efficacy and safety of activation stimuli used in clinical IVF and will make it possible for the first time to ascertain the impact of Ca²⁺ oscillations on gene expression in the early embryo and on the health of offspring.

A key role of the sperm-induced Ca²⁺ oscillations is to downregulate, via a signalling pathway involving CamKIIγ and Emi2, MPF, which is responsible for the metaphase II arrest of the egg (Fig. S2A) (Sanders and Swann, 2016; Sobinoff et al., 2013). A later decline in MAPK activity correlates with the formation of pronuclei and entry into interphase of the first cell cycle. Importantly, MPF levels can be reduced artificially in various ways, even without a Ca²⁺ stimulus, triggering egg activation and development to blastocyst *in vitro* (Knott et al., 2006; Miao et al., 2012; Phillips et al., 2002; Suzuki et al., 2010).

This mode of egg activation, without Ca²⁺ release, may explain the spontaneous activation observed *in vivo* in ovulated hamster and mouse eggs left to reside in the oviduct for extended periods of time in the absence of fertilization (Whittingham and Siracusa, 1978; Xu et al., 1997; Yanagimachi and Chang, 1961). Moreover, eggs from the C57BL/6 strain, the strain used in our studies, have been shown to have a particularly high susceptibility to spontaneous activation during *in vitro* maturation (Cheng et al., 2012). Thus, it is possible that a related mechanism might be responsible for the activation we observe. In the situation described here, the self-activation that aging unfertilized eggs experience, which normally results in fragmentation or embryonic arrest, is rescued by the *Plcz1*⁻ fertilizing sperm. It remains to be seen if these findings have relevance for other mammals, including humans, besides mice.

One other possibility is that *Plcz1*⁻ sperm are inducing an atypical Ca²⁺ signal in the egg, which was not detected during the 4 h window during which Ca²⁺ monitoring was performed in our IVF studies. However, we failed to detect any form of Ca²⁺ response following ICSI or IVF with *Plcz1*⁻ sperm. Furthermore, following IVF or *in vivo* fertilization, there was a marked increase in the rates of polyspermy, which suggest that the fertilizing sperm cannot induce Ca²⁺ release to engage the mechanisms that block polyspermy. Last, a final formal possibility is that sperm factors other than PLCζ might be involved in egg activation in this instance. The post-acrosomal sheath WW domain-binding protein (PAWP) has been suggested to play a role in egg activation (Aarabi et al., 2014). However, sperm from PAWP-null (*Wbp2nt*^{-/-}) mice have no defect in egg activation capacity (Satouh et al., 2015), arguing against a role in this process. Future studies will be required to uncover which of these potential



Our findings are important in this respect in two main ways. First, our demonstration that *Plcz1*^{-/-} mouse males can still conceive offspring *in vivo*, albeit at a reduced efficiency, seemingly in the absence of the normal sperm-induced Ca²⁺ oscillations, will allow us to study whether these offspring differ from those resulting from normal egg activation that is dependent on Ca²⁺ signals. Second, the availability of PLCζ-null sperm now makes it possible to assess, in a mouse model, how artificial egg activation stimuli, used in the clinic, might affect embryonic gene expression and offspring growth, metabolism and behaviour. Importantly, it will provide a way to test the efficacy and safety of recombinant PLCζ protein as an alternative therapeutic agent to treat infertility caused by egg activation deficiency.

Mice

At the University of Massachusetts and the University of Ghent Hospital Medical School, mice were also used as a source of eggs for ICSI, IVF and microinjection experiments. Sperm used in these experiments were cryopreserved using straws at the University of Oxford and sent to the Massachusetts and Ghent labs where they were thawed before use in the experiments.

In Ghent, mice used for egg collection were 8- to 10-week-old B6D2F1 females (a cross between female C57BL/6 and male DBA/2 mice). All procedures involving live-animal handling and euthanasia were approved by

There has been considerable debate about the importance of Ca^{2+} oscillations for optimal egg activation and subsequent embryo development. Although it is possible to bypass the Ca^{2+} -dependent route *in vitro* in various ways (Knott et al., 2006; Miao et al., 2012; Phillips et al., 2002; Suzuki et al., 2010), altering the number and frequency of Ca^{2+} transients can subtly affect embryonic gene

Table 1. Fertility parameters

Crosses			Number of litters born (10-week period)	Litter size (average±s.e.m.)	Pups/breeding female (10-week period)	Genotype ratio (%) (wild type/Mut/Het)
Male	×	Female				
Wild type (n=7)	×	Wild type (n=8)	13	7.8±0.8	12.7±1.8	
Het ^(em1Jparr) (n=3)	×	Het ^(em1Jparr) (n=4)	9	4.7±1.1 ^{ns}	10.5±0.9 ^{ns}	21.1/23.1/55.8
Het ^(em2Jparr) (n=4)	×	Het ^(em2Jparr) (n=6)	13	7.1±0.5 ^{ns}	15.3±0.9 ^{ns}	27.6/25.8/46.4
Het ^(em1Jparr) (n=4)	×	Mut ^(em1Jparr) (n=8)	17	5.7±0.6 ^{ns}	12.1±2.5 ^{ns}	
Het ^(em2Jparr) (n=3)	×	Mut ^(em2Jparr) (n=4)	8	4.9±0.7 ^{ns}	9.7±2.3 ^{ns}	
Mut ^(em1Jparr) (n=4)	×	Wild type (n=7)	8	4.2±0.6*	4.9±1.2**	
Mut ^(em2Jparr) (n=6)	×	Wild type (n=7)	5	3.2±1.2*	2.3±1.0***	

Mating pairs or trios were set up between males and females with genotypes as indicated. Data refer to pups born during the initial 10 weeks of mating and are presented as average±s.e.m. followed by analysis using one-way ANOVA.

ns, not significant; * $P<0.05$; ** $P<0.01$; *** $P<0.001$.

Het, *Plcz1*^{+/em1Jparr} or *Plcz1*^{+/em2Jparr}.

Mut, homozygote *Plcz1*^{em1Jparr} or *Plcz1*^{em2Jparr}.

Wild type, homozygote *Plcz1*^{WT}.

the Ghent University Hospital Ethical Committee for Laboratory Animals (EC number 09/15).

sgRNA design and production

Single guide RNA (sgRNA) target sites were selected within the mouse *Plcz1* sequence (NM_054066.4) using the CRISPR design tool (crispr.mit.edu). sgRNA sequences were cloned into either pX459 (Cas9^{WT}) or pX461 (Cas9^{D10A}) vectors (gifts from Prof. Feng Zhang, Massachusetts Institute of Technology, USA) and tested for efficacy by transfection into N2A mouse neuroblastoma cells using Eugene 6 followed by High Resolution Melting (HRM) analysis (Bassett and Liu, 2014). N2A mouse neuroblastoma cells were tested for mycoplasma, and were originally obtained from ATCC (https://www.lgcstandards-atcc.org/products/all/CCL-131.aspx?geo_country=gb). Based on HRM results, a pair of targeting sequences in exon 3 (GTATGAAGCACGaGAAGTTAAGG, AAGGTTCAAGGATGATTTAGAGG) and a single targeting sequencing in exon 5 (ACTCGGTCCCAATATTTGATCGG) were chosen for production of sgRNAs by *in vitro* transcription using a PCR template generated by Pfu polymerase extension of a pair of overlapping primers, which add a T7 polymerase promoter (underlined) to the 5' end and the common sgRNA sequence (bold) to the 3' end: PLCZ1_exon3A(F), gaaattaatacagactcactataggAGGTTCAGGATGATTTAGGtttttagagctagaataatagc; PLCZ1_exon3B(F), gaaattaatacagactcactataggTATGAAGCACGaGAAGTTAgttttagagctagaataatagc; PLCZ1_exon5(F), gaaattaatacagactcactataggCTCGGTCCCAATATTTGATgttttagagctagaataatagc; sgRNA (R), aaaagcaccgactcggtgccattttcaagtgataacggactagcctatttttaactgtctatttctagctctaaaac.

Products were purified using a PCR purification kit (Qiagen), and *in vitro* transcribed using the T7 MEGascript kit (Ambion) at 37°C for 4 h. sgRNAs were purified by phenol:chloroform extraction and precipitation using isopropanol followed by quantification by measuring absorbance at 260 nm. Total sgRNA (5 µg) was mixed with 10 µg capped and polyadenylated Cas9^{WT} or Cas9^{D10A} mRNA (Trilink) and 0.1 volumes 3 M sodium acetate (pH 5.2), and co-precipitated using three volumes ethanol. RNA was washed twice in 70% ethanol and resuspended in 15 µl water to a concentration of 1 mg/ml. Integrity of mRNA and sgRNA was confirmed by agarose gel electrophoresis.

Generation of *Plcz1*^{-/-} mice

Three- to 4-week-old C57BL/6J female mice (Charles River) were injected intraperitoneally with 5 IU of PMSG (Intervet) and 48 h later with 5 IU of hCG (Intervet), and were paired with C57BL/6J (Charles River) male mice. Zygotes were retrieved from oviductal ampullae at 20 h post-hCG. Cumulus-enclosed zygotes were denuded by exposure to 1 mg/ml hyaluronidase (Sigma) in modified human tubule fluid (HTF) (Zenith Biotech) for 3-6 min, washed through fresh modified HTF and cultured in HTF in the presence of 5% CO₂ at 37°C. Two hours after release from the cumulus mass, zygotes with a normal morphology were microinjected into the cytoplasm in 30 µl drops of modified HTF media using a PMM-150FU Piezo impact drive (Primetech) with homemade glass capillaries with ~5-10 pL RNA at a final concentration of 150 ng/µl (100 ng/µl Cas9 cRNA and 50 ng/µl sgRNA).

Injected zygotes and non-injected controls were cultured overnight in KSOMaa (Zenith Biotech) in the presence of 5% CO₂ at 37°C and checked for two-cell division the next day. B6CBF1 females (Charles River) were mated to a vasectomized male, and females showing the presence of a copulatory plug were surgically prepared to receive all zygotes with a normal two-cell morphology using a bilateral implantation. The resulting F0 offspring were biopsied, their genomic DNA was analysed by HRM, PCR products were cloned into PGEM-T vector and individual clones were sequenced. Founder F0 mice with mutant alleles were bred to C57BL/6J mice and offspring were tested for inheritance of mutant alleles by DNA sequencing. Heterozygote progeny (*Plcz1*^{+/-}) were mated for production of homozygote mice (*Plcz1*^{-/-}) and a colony for each *Plcz1* mutant line was maintained by mating pairs using *Plcz1*^{-/-} females and *Plcz1*^{+/-} males.

Genotyping of *Plcz1* mutant lines by PCR

Genomic DNA was extracted from tail or ear biopsies by digestion with proteinase K overnight at 65°C with agitation in 0.5 ml lysis buffer [100 mM Tris-HCl (pH 8), 5 mM EDTA, 200 mM NaCl, 0.1% SDS, 0.5 mg/ml proteinase K (Roche)]. Extracts were centrifuged at 17,000 g for 4 min, and supernatant was diluted 6.5× into water prior to inactivation of proteinase K at 95°C for 10 min. A 1 µl sample was used as a template for 10 µl PCR reactions using the following primers: *Plcz1*^{em1Jparr} (F, ACAGGCAGGGAAAGGGTTT; R, TGTCTGAGCACAGGATAGATGA; wild-type product, 266 bp; mutant product, 244 bp); *Plcz1*^{em2Jparr} (F, AGAAAGAAGGGAGGGGAATCTTC; R, TGATGGTATATCTGCATCC-TTCTT; wild-type product, 342 bp; mutant product, 325 bp). Products were analysed by gel electrophoresis and by DNA sequencing.

Analysis of *Plcz1* and *Wbp2nl* mRNA expression in testis

Total RNA was extracted from testes using single-step RNeasy RT (Sigma). For *Plcz1* mRNA expression analysis, conventional RT-PCR was performed on the total RNA using OneTaq One-Step RT-PCR (New England Biolabs). The primers used to analyse *Plcz1* mRNA expression, which are designed to anneal in different exons, were: *Plcz1*^{em1Jparr} (F, AAGCCAACCTTCATGAGCTCG; R, TCAATGGTGATTCTTCTTGGT; wild-type product, 192 bp; mutant product, 170 bp); *Plcz1*^{em2Jparr} (F, GA-GAACTGTAAAACCGTGATACCA; R, CCCAGCAGTCAATTTCCAGA; wild-type product, 172 bp; mutant product, 155 bp).

Products were analysed by gel electrophoresis and by DNA sequencing. *Wbp2nl* mRNA expression levels were quantified in testes RNA by using OnestepPLUS qRT-PCR MasterMix SYBR Green (Primerdesign).

The primers used for *Wbp2nl* mRNA detection were: F, GGCAGCTC-CAGACGGTGGCT; R, GCCCATCCAGAAGCTTGCAACTCG.

Wbp2nl mRNA expression levels were normalized to β-actin mRNA expression levels, and calculated using the relative quantification approach. Real-time qPCR was performed on a Roche LightCycler 480.

Immunoblot analysis of PLCζ and PAWP in sperm

Immunoblotting was performed as previously published (Kurokawa et al., 2005). Mouse sperm were diluted to appropriate concentrations, 2× sample

buffer was added and samples were kept at -80°C until use. Thawed samples were boiled for 3 min, mixed well and loaded onto 7.5% SDS-PAGE gels; resolved polypeptides were transferred onto PVDF membranes (Millipore) using a Mini Trans-Blot Cell (Bio-Rad). The membranes were blocked in 6% nonfat dry milk in PBS-0.1% Tween and incubated overnight at 4°C with 1/1000 dilution of a custom-made anti-PLC ζ rabbit sera [raised against a 19-mer sequence (GYRRVPLFSKSGANLEPSS) at the C-terminus of mouse PLC ζ (mPLC ζ)]; this was followed by a 1 h incubation with 1/2000 of a goat anti-rabbit horseradish peroxidase-labelled secondary antibody (Bio-Rad, 1662408EDU). Immunoreactivity was detected using chemiluminescence according to the manufacturer's instructions (PerkinElmer) using a Kodak Image Station 440CF. Immunoblot analysis of WPB2NL/PAWP was performed in a similar way, using overnight incubation at 4°C with 1/1000 dilution of an anti-WPB2NL/PAWP rabbit polyclonal antibody (Proteintech-22587-1-AP) (Kashir et al., 2017); this was followed by 1 h of incubation with 1/15,000 dilution of a goat anti-rabbit IRDye-800CW secondary antibody (Li-Cor, 926-32211) and fluorescence imaged using a Li-Cor Odyssey imaging system (Li-Cor). Immunoblotting procedures were repeated at least three times per sample.

Generation of recombinant PLC ζ 1 RNA

A synthetic mouse *Plcz1* cDNA (GeneArt Gene Synthesis, ThermoFisher Scientific) was subcloned into a pRNA vector for production of polyA⁺/capped recombinant mRNA using T3 RNA polymerase in an *in vitro* transcription reaction; capped transcripts were produced with the cap analogue m⁷G(5')ppp(5')G, following the manufacturer's instructions (mMessage mMachine, Ambion). Mutant *Plcz1* cDNA versions were obtained by swapping internal fragments within wild-type *Plcz1* cDNA, with corresponding synthetic sequences harbouring the deletions present in *Plcz1*^{em1Jparr} or *Plcz1*^{em2Jparr}. The quality of the recombinant mRNA was assessed by agarose gel electrophoresis.

Histology

Testes were fixed in 4% paraformaldehyde (PFA), dehydrated in increasing concentrations of ethanol, kept for 24 h in Histo-Clear II (National Diagnostics), then embedded in paraffin wax. Sections (5 μm) were cut and mounted on Superfrost Plus slides (Fisher Scientific). The sections were deparaffinized in Histo-Clear II, rehydrated in decreasing concentrations of ethanol, then stained with Harris Hematoxylin (Sigma-Aldrich) for 5 min. The sections were counterstained with eosin B solution (Sigma-Aldrich) and visualized under a Leica DM5000B microscope.

Sperm viability

Spermatozoa were collected from the cauda epididymis and vas deferens of 8-week-old mice and incubated in HEPES-buffered saline solution containing 4 mg/ml bovine serum albumin at 37°C for 30 min, and assayed using the LIVE/DEAD Sperm Viability Kit (Molecular Probes) following the manufacturer's instructions. In brief, the samples were incubated for 5 min with SYBR14 (Em 516 nm; labels live cells) at a final concentration of 100 nM, and then with PI (Em 617 nm; labels dead cells) at a final concentration of 12 μM for another 5 min. Stained samples were analysed using a BD FACS Canto II flow cytometer equipped with BD FACSDiva software version 6.1 collecting a minimum of 10,000 gated sperm cells for the log of the fluorescence. Samples within the SYBR14⁺/PI⁻ quadrant were considered viable, and within the SYBR14⁻/PI⁺ quadrant were non-viable. Events within the SYBR14⁺/PI⁻ quadrant were considered as debris. Data were analysed for the relative fluorescence of SYBR14/PI using FlowJo software v10.6. Sperm viability was calculated by the percentage of live cells relative to the total number. Images of fluorescently labelled sperm were obtained from samples loaded onto a microscope slide coated with 0.1% poly-D-lysine and imaged using an Olympus BX40 microscope.

Sperm motility and hyperactivation

Spermatozoa were collected as before and washed in a complete pre-warmed HTF medium at 37°C under 5% CO₂. A 30 μl sample of the recovered sperm suspension (2×10^5 sperm/ml) after 1 h incubation with HTF was loaded into

a pre-warmed Leja slide chamber by capillary action on an Olympus CX41 microscope. Sperm motility and hyperactivation parameters were analysed using computer-assisted sperm analysis (CASA) with software HTM-CEROS (version 12.3, Hamilton Thorne), recording at least 800 mouse sperm/slide for each group. The image-acquiring settings were: 60 frames per second, minimum contrast (50), minimum cell size (10 pixels), VAP cutoff (7.5 $\mu\text{m/s}$), VSL cutoff (6 $\mu\text{m/s}$), cell intensity (80). Different progressive sperm motility grading scores (rapid, medium, slow, static) were recorded according to the Average Path Velocity (VAP) and Straight Line Velocity (VSL) parameters, while sperm hyperactivation (vigour) values were evaluated by Curvilinear Velocity (VCL), Amplitude of Lateral Head displacement (ALH) and Beat Cross Frequency (BCF).

Acrosome reaction

Spermatozoa were collected as before, washed, then capacitated in complete HTF medium for 30 min at 37°C and 5% CO₂. The samples were divided into three groups at a sperm density of 3×10^6 sperm/ml: the first group was treated with ionomycin at a final concentration of 10 μM in DMSO, the second group was treated with progesterone at a final concentration of 20 μM in DMSO and the third group was only treated with DMSO as a control. At different time points, spermatozoa were collected and pipetted onto a microscope slide coated with 0.1% poly-d-lysine, then fixed with acetone/methanol (1:1) on ice for 10 min. The slides were washed twice with phosphate-buffered saline before incubating with lectin PNA-Alexa Fluor 594 conjugate (Life Technologies) for 30 min in the dark. Slides were washed twice with H₂O before mounting with ProLong Gold antifade reagent with DAPI for sperm DNA staining. The slides were assessed for acrosomal status (lectin PNA⁺, unreacted; lectin PNA⁻, reacted) using an Olympus BX40 microscope. The percentage of acrosome-reacted spermatozoa was calculated as percentage of total numbers.

Intracytoplasmic sperm injection (ICSI)

ICSI was carried out both at the University of Ghent Hospital Medical School and at the University of Massachusetts. Briefly, hybrid female mice were stimulated using pregnant mare serum gonadotrophin (PMSG). MII eggs were obtained from the oviducts 12 to 14 h after injection of hCG. After treatment with hyaluronidase to remove cumulus cells, MII eggs were washed and transferred into KSOM (potassium simplex optimized medium) under culture conditions (37°C , 6% CO₂, 5% O₂). Sperm microinjection was performed by piezo-drilling following protocols previously described (Yoshida and Perry, 2007; Yoon and Fissore, 2007). All manipulations were carried out using HEPES-buffered medium at 37°C , under light mineral oil at room temperature. Sperm heads were separated from the tail and microinjected by applying Piezo pulses of different intensity to penetrate the zona pellucida and plasma membrane of the egg. The sperm head was then released into the ooplasm and the pipette carefully withdrawn from the egg.

In vitro fertilization and zona pellucida-free eggs

Mouse eggs were collected as above and as previously described following standard superovulation procedures (Navarrete et al., 2015). Up to four cumulus-oocyte complexes (COCs) were placed into a 90 μl drop of media (TYH standard medium) covered with mineral oil and previously equilibrated in an incubator with 5% CO₂ at 37°C . Fertilization drops containing 20–30 eggs were inseminated with sperm from each genotype incubated as described above in medium supporting capacitation (final concentration of 1×10^6 cells/ml). Fertilization and polyspermy were evaluated using Hoechst staining at different hours post-insemination. In the case where [Ca²⁺]_i monitoring was performed, following egg collection the zonae pellucidae were removed using acidic Tyrode's solution (pH 1.6) (Bernhardt et al., 2015). Zona pellucida-free eggs were adhered to Cell-Tak (MatTek)-treated glass-bottom dishes in 90 μl BSA-free TYH, and sperm were added to a final concentration of 10^5 sperm/ml, along with 4 μl TYH containing 30 mg/ml BSA for a final concentration of ~ 1.5 mg/ml BSA. Imaging began immediately after sperm addition and was performed essentially as described below. Because the sperm from both *Plcz1*^{-/-} males was cryopreserved, the control sperm was also cryopreserved and it was collected from a transgenic mouse line originally generated by Dr G. S. McKnight (University of Washington, WA, USA) (Morgan et al.,

2008). Sperm penetration was confirmed by the presence of Ca^{2+} responses, as the large number of frozen sperm needed to achieve fertilization made it impossible to assess sperm entry.

Sperm penetration

Sperm-egg penetration analysis was performed 6 h post-*in vitro* fertilization. Briefly, C57BL/6J female mice at 3-4 weeks old (Charles River) were stimulated using 5 IU pregnant mare serum gonadotrophin (PMSG, Folligon, Intervet). Ovulation was induced 46-48 h later using 5 IU hCG (Chorulon, Intervet). Oocyte-granulosa cell complexes (MII eggs) were collected 13-14 h following hCG administration in a complete pre-warmed HTF medium (Zenith Biotech), and then inseminated with pre-capacitated sperm from each animal group under mineral oil (Zenith Biotech) at 37°C and 5% CO_2 . Six hours later, eggs were washed and treated for 60 s with acid Tyrode's solution to remove the extra sperm attached to the zona pellucida. The eggs were then fixed in 3.7% paraformaldehyde for 30 min, and washed and permeabilized before DNA staining with Hoechst 33324. Sperm DNA was detected using a 358/461 (ex/em.) laser line on a LSX8 Leica confocal scanning laser microscope. High-resolution image series on *z* plane were generated in order to build 3-dimensional (3D) images of the embryos. Counting of sperm heads inside the eggs confirmed by the DNA staining method, was carried out on 3D projections. Processing and analysis of the digital images were performed using Image-J/Fiji.

Microinjection of *PLCz1* cRNA

Microinjections were performed as described previously (Lee et al., 2016). cRNA was prepared as previously described and 1-2 µl used to prepare micro drops from which glass micropipettes were loaded by aspiration. cRNAs were delivered into eggs and/or zygotes by pneumatic pressure (PLI-100 picoinjector, Harvard Apparatus). Each egg received 5-10 pl, ~1-3% of the total volume of the egg. Injection of cRNA into zygotes was performed 3 h after completion of ICSI.

Calcium imaging

This was carried out in two different ways. Using one approach, eggs were pre-incubated for 30 min at 37°C in KSOM containing the Ca^{2+} -sensitive fluorescent dye Fura-2 acetoxymethyl ester (7.5 µM) (Fura-2 AM, Invitrogen). After ICSI, eggs were transferred to a 10 µl KSOM droplet in a glass dish (MatTek) for Ca^{2+} analysis. Imaging was performed on an inverted epifluorescence microscope (Nikon Eclipse TE 300, Analis) using a 20× objective and filter switch (Lambda DG-4 filter switch, Sutter Instrument), for excitation at 340 and 380 nm corresponding to Fura-2 AM spectrum. Images were acquired every 5 s for a duration of 2 h and intracellular Ca^{2+} changes were registered as the ratio of fluorescence (340/380 nm). In another approach, $[\text{Ca}^{2+}]_i$ monitoring was performed as previously described (Lee et al., 2016), also using Fura 2-AM.

In vitro development of *in vivo* fertilized eggs

Three- to 4-week-old C57BL/6J female mice (Charles River) were injected intraperitoneally with 5 IU of PMSG (Intervet) and 48 h later with 5 IU of hCG (Intervet), and paired with male mice. Zygotes were retrieved from oviductal ampullae at 18 h post-hCG. Cumulus-enclosed zygotes were denuded by exposure to 1 mg/ml hyaluronidase (Sigma) in modified HTF (Zenith Biotech) for 3-6 min, washed through fresh modified HTF and cultured in KSOMaa in the presence of 5% CO_2 at 37°C. For assessment of polyspermy, denuded and washed zygotes were cultured in KSOMaa in the presence of 5% CO_2 at 37°C for 30 min. The zygotes were then placed in fresh modified HTF containing 1 µg/ml Hoechst 33342 and incubated for 20-30 min. They were washed in fresh modified HTF and imaged using a fluorescence microscope.

Statistical analyses

Where indicated, data are presented as average±s.e.m. and analysed by a one-way ANOVA with Bonferroni's or Tukey's multiple comparison tests, or Student's *t*-test, as appropriate. In some figures, data are presented as the proportion of total eggs examined showing a specific characteristic from combined experiments; contingency tables with a Fisher's exact test were

used in these cases. Graphs are annotated with the following conventions: ns, $P>0.05$; * $P<0.05$; ** $P<0.01$; *** $P<0.001$.

Acknowledgements

We thank the technical staff of the University of Oxford, University of Massachusetts, and the University of Ghent Hospital Medical School, for their help in breeding and maintaining the mice used in this study.

Competing interests

The authors declare no competing or financial interests.

Author contributions

Conceptualization: A.H., J.G., M.R., H.C.L., M.F.B., G.A., A.B., S.F., F.N., B.H., R.F., J.P.; Methodology: A.H., J.G., M.R., H.C.L., M.F.B., G.A., A.B., S.F., F.N., B.H., R.F., J.P.; Validation: A.H., J.G., M.R., H.C.L., M.F.B., G.A., A.B., S.F., F.N.; Formal analysis: J.G., M.R., H.C.L., M.F.B., G.A., A.B., S.F., F.N.; Investigation: A.H., J.G., M.R., H.C.L., M.F.B., G.A., A.B., S.F., F.N.; Data curation: A.H., J.G., M.R., H.C.L., M.F.B., G.A., A.B., S.F., F.N.; Writing - original draft: J.P.; Writing - review & editing: M.R., B.H., R.F., J.P.; Supervision: P.d.S., B.H., R.F., J.P.; Project administration: J.P.; Funding acquisition: P.d.S., B.H., R.F., J.P.

Funding

Work in J.P.'s lab was funded by a DPhil grant to A.H. from the Iraqi Higher Committee for Education Development and by an Academic Scholarship Award grant from the Society for Reproduction and Fertility. Work in B.H.'s and P.d.S.'s labs was funded by a project funding grant from the Fonds Wetenschappelijk Onderzoek (FWO) (G060615N) and by a fundamental clinical research mandate from FWO to P.d.S. Work in R.F.'s lab was funded by a National Institutes of Health grant (HD051872). Deposited in PMC for release after 12 months.

Supplementary information

Supplementary information available online at <http://dev.biologists.org/lookup/doi/10.1242/dev.150227.supplemental>

References

- Aarabi, M., Yu, Y., Xu, W., Tse, M. Y., Pang, S. C., Yi, Y.-J., Sutovsky, P. and Oko, R. (2012). The testicular and epididymal expression profile of PLCzeta in mouse and human does not support its role as a sperm-borne oocyte activating factor. *PLoS ONE* **7**, e33496.
- Aarabi, M., Balakier, H., Bashar, S., Moskovtsev, S. I., Sutovsky, P., Librach, C. L. and Oko, R. (2014). Sperm-derived WW domain-binding protein, PAWP, elicits calcium oscillations and oocyte activation in humans and mice. *FASEB J.* **28**, 4434-4440.
- Bassett, A. and Liu, J.-L. (2014). CRISPR/Cas9 mediated genome engineering in *Drosophila*. *Methods* **69**, 128-136.
- Bernhardt, M. L., Lowther, K. M., Padilla-Banks, E., McDonough, C. E., Lee, K. N., Evsikov, A. V., Uliasz, T. F., Chidiac, P., Williams, C. J. and Mehlmann, L. M. (2015). Regulator of G-protein signaling 2 (RGS2) suppresses premature calcium release in mouse eggs. *Development* **142**, 2633-2640.
- Bianchi, E., Doe, B., Goulding, D. and Wright, G. J. (2014). Juno is the egg Izumo receptor and is essential for mammalian fertilization. *Nature* **508**, 483-487.
- Cheng, Y., Zhong, Z. and Latham, K. E. (2012). Strain-specific spontaneous activation during mouse oocyte maturation. *Fertil. Steril.* **98**, 200-206.
- Doudna, J. A. and Charpentier, E. (2014). Genome editing. The new frontier of genome engineering with CRISPR-Cas9. *Science* **346**, 1258096.
- Ducibella, T., Huneau, D., Angelichio, E., Xu, Z., Schultz, R. M., Kopf, G. S., Fissore, R., Madoux, S. and Ozil, J.-P. (2002). Egg-to-embryo transition is driven by differential responses to Ca^{2+} oscillation number. *Dev. Biol.* **250**, 280-291.
- Escoffier, J., Lee, H. C., Yassine, S., Zouari, R., Martinez, G., Karaouzen, T., Coutton, C., Kherraf, Z.-E., Halouani, L., Triki, C. et al. (2016). Homozygous mutation of PLCZ1 leads to defective human oocyte activation and infertility that is not rescued by the WW-binding protein PAWP. *Hum. Mol. Genet.* **25**, 878-891.
- Ferrer-Vaquer, A., Barragan, M., Freour, T., Vernaev, V. and Vassena, R. (2016). PLCzeta sequence, protein levels, and distribution in human sperm do not correlate with semen characteristics and fertilization rates after ICSI. *J. Assist. Reprod. Genet.* **33**, 747-756.
- Heytens, E., Parrington, J., Coward, K., Young, C., Lambrecht, S., Yoon, S.-Y., Fissore, R. A., Hamer, R., Deane, C. M., Ruas, M. et al. (2009). Reduced amounts and abnormal forms of phospholipase C zeta (PLCzeta) in spermatozoa from infertile men. *Hum. Reprod.* **24**, 2417-2428.
- Igusa, Y. and Miyazaki, S. (1986). Periodic increase of cytoplasmic free calcium in fertilized hamster eggs measured with calcium-sensitive electrodes. *J. Physiol.* **377**, 193-205.
- Ito, J., Parrington, J. and Fissore, R. A. (2011). PLCzeta and its role as a trigger of development in vertebrates. *Mol. Reprod. Dev.* **78**, 846-853.

- Kashir, J., Jones, C., Lee, H. C., Rietdorf, K., Nikiforaki, D., Durrans, C., Ruas, M., Tee, S. T., Heindryckx, B., Galione, A. et al. (2011). Loss of activity mutations in phospholipase C zeta (PLCzeta) abolishes calcium oscillatory ability of human recombinant protein in mouse oocytes. *Hum. Reprod.* **26**, 3372-3387.
- Kashir, J., Konstantinidis, M., Jones, C., Lemmon, B., Lee, H. C., Hamer, R., Heindryckx, B., Deane, C. M., De Sutter, P., Fissore, R. A. et al. (2012). A maternally inherited autosomal point mutation in human phospholipase C zeta (PLCzeta) leads to male infertility. *Hum. Reprod.* **27**, 222-231.
- Kashir, J., Buntwal, L., Nomikos, M., Calver, B. L., Stamatiadis, P., Ashley, P., Vassilakopoulou, V., Sanders, D., Knaggs, P., Livanou, E. et al. (2017). Antigen unmasking enhances visualization efficacy of the oocyte activation factor, phospholipase C zeta, in mammalian sperm. *Mol. Hum. Reprod.* **23**, 54-67.
- Kline, D. and Kline, J. T. (1992). Repetitive calcium transients and the role of calcium in exocytosis and cell cycle activation in the mouse egg. *Dev. Biol.* **149**, 80-89.
- Knott, J. G., Kurokawa, M., Fissore, R. A., Schultz, R. M. and Williams, C. J. (2005). Transgenic RNA interference reveals role for mouse sperm phospholipase C zeta in triggering Ca²⁺ oscillations during fertilization. *Biol. Reprod.* **72**, 992-996.
- Knott, J. G., Gardner, A. J., Madgwick, S., Jones, K. T., Williams, C. J. and Schultz, R. M. (2006). Calmodulin-dependent protein kinase II triggers mouse egg activation and embryo development in the absence of Ca²⁺ oscillations. *Dev. Biol.* **296**, 388-395.
- Kurokawa, M., Sato, K., Wu, H., He, C., Malcuit, C., Black, S. J., Fukami, K. and Fissore, R. A. (2005). Functional, biochemical, and chromatographic characterization of the complete [Ca²⁺]_i oscillation-inducing activity of porcine sperm. *Dev. Biol.* **285**, 376-392.
- Lee, H. C., Yoon, S.-Y., Lykke-Hartmann, K., Fissore, R. A. and Carvacho, I. (2016). TRPV3 channels mediate Ca²⁺(+) influx induced by 2-APB in mouse eggs. *Cell Calcium* **59**, 21-31.
- Li, L., Lu, X. and Dean, J. (2013). The maternal to zygotic transition in mammals. *Mol. Aspects Med.* **34**, 919-938.
- Miao, Y.-L., Stein, P., Jefferson, W. N., Padilla-Banks, E. and Williams, C. J. (2012). Calcium influx-mediated signaling is required for complete mouse egg activation. *Proc. Natl. Acad. Sci. USA* **109**, 4169-4174.
- Morgan, D. J., Weisenhaus, M., Shum, S., Su, T., Zheng, R., Zhang, C., Shokat, K. M., Hille, B., Babcock, D. F. and McKnight, G. S., (2008). Tissue-specific PKA inhibition using a chemical genetic approach and its application to studies on sperm capacitation. *Proc. Natl. Acad. Sci. USA* **105**, 20740-20745.
- Navarrete, F. A., García-Vázquez, F. A., Alvau, A., Escoffier, J., Krapf, D., Sánchez-Cárdenas, C., Salicioni, A. M., Darszon, A. and Visconti, P. E. (2015). Biphasic role of calcium in mouse sperm capacitation signaling pathways. *J. Cell. Physiol.* **230**, 1758-1769.
- Nomikos, M., Kashir, J., Swann, K. and Lai, F. A. (2013). Sperm PLCzeta: from structure to Ca²⁺ oscillations, egg activation and therapeutic potential. *FEBS Lett.* **587**, 3609-3616.
- Ozil, J.-P., Markoulaki, S., Toth, S., Matson, S., Banrezes, B., Knott, J. G., Schultz, R. M., Huneau, D. and Ducibella, T. (2005). Egg activation events are regulated by the duration of a sustained [Ca²⁺]_{cyt} signal in the mouse. *Dev. Biol.* **282**, 39-54.
- Parrington, J., Davis, L. C., Galione, A. and Wessel, G. (2007). Flipping the switch: how a sperm activates the egg at fertilization. *Dev. Dyn.* **236**, 2027-2038.
- Phillips, K. P., Petrunewich, M. A. F., Collins, J. L., Booth, R. A., Liu, X. J. and Baltz, J. M. (2002). Inhibition of MEK or cdc2 kinase parthenogenetically activates mouse eggs and yields the same phenotypes as Mos(-/-) parthenogenotes. *Dev. Biol.* **247**, 210-223.
- Ran, F. A., Hsu, P. D., Lin, C.-Y., Gootenberg, J. S., Konermann, S., Trevino, A. E., Scott, D. A., Inoue, A., Matoba, S., Zhang, Y. et al. (2013). Double nicking by RNA-guided CRISPR Cas9 for enhanced genome editing specificity. *Cell* **154**, 1380-1389.
- Sanders, J. R. and Swann, K. (2016). Molecular triggers of egg activation at fertilization in mammals. *Reproduction* **152**, R41-R50.
- Sanusi, R., Yu, Y., Nomikos, M., Lai, F. A. and Swann, K. (2015). Rescue of failed oocyte activation after ICSI in a mouse model of male factor infertility by recombinant phospholipase C zeta. *Mol. Hum. Reprod.* **21**, 783-791.
- Satouh, Y., Nozawa, K. and Ikawa, M. (2015). Sperm postacrosomal WW domain-binding protein is not required for mouse egg activation. *Biol. Reprod.* **93**, 94.
- Saunders, C. M., Larman, M. G., Parrington, J., Cox, L. J., Royse, J., Blayney, L. M., Swann, K. and Lai, F. A. (2002). PLC zeta: a sperm-specific trigger of Ca²⁺ oscillations in eggs and embryo development. *Development* **129**, 3533-3544.
- Sfontouris, I. A., Nastri, C. O., Lima, M. L. S., Tahmasbpourmarzouni, E., Raine-Fenning, N. and Martins, W. P. (2015). Artificial oocyte activation to improve reproductive outcomes in women with previous fertilization failure: a systematic review and meta-analysis of RCTs. *Hum. Reprod.* **30**, 1831-1841.
- Shen, B., Zhang, W., Zhang, J., Zhou, J., Wang, J., Chen, L., Wang, L., Hodgkins, A., Iyer, V., Huang, X. et al. (2014). Efficient genome modification by CRISPR-Cas9 nickase with minimal off-target effects. *Nat. Methods* **11**, 399-402.
- Sobinoff, A. P., Sutherland, J. M. and McLaughlin, E. A. (2013). Intracellular signalling during female gametogenesis. *Mol. Hum. Reprod.* **19**, 265-278.
- Suzuki, T., Yoshida, N., Suzuki, E., Okuda, E. and Perry, A. C. F. (2010). Full-term mouse development by abolishing Zn²⁺-dependent metaphase II arrest without Ca²⁺ release. *Development* **137**, 2659-2669.
- Swann, K. and Lai, F. A. (2016). The sperm phospholipase C-zeta and Ca²⁺ signalling at fertilization in mammals. *Biochem. Soc. Trans.* **44**, 267-272.
- Vanden Meerschaut, F., Nikiforaki, D., Heindryckx, B. and De Sutter, P., (2014). Assisted oocyte activation following ICSI fertilization failure. *Reprod. Biomed. Online* **28**, 560-571.
- Wakai, T., Vanderheyden, V. and Fissore, R. A. (2011). Ca²⁺ signaling during mammalian fertilization: requirements, players, and adaptations. *Cold Spring Harb. Perspect. Biol.* **3**, a006767.
- Whittingham, D. G. and Siracusa, G. (1978). The involvement of calcium in the activation of mammalian oocytes. *Exp. Cell Res.* **113**, 311-317.
- Xu, Z., Abbott, A., Kopf, G. S., Schultz, R. M. and Ducibella, T. (1997). Spontaneous activation of ovulated mouse eggs: time-dependent effects on M-phase exit, cortical granule exocytosis, maternal messenger ribonucleic acid recruitment, and inositol 1,4,5-trisphosphate sensitivity. *Biol. Reprod.* **57**, 743-750.
- Yanagimachi, R. and Chang, M. C. (1961). Fertilizable life of golden hamster ova and their morphological changes at the time of losing fertilizability. *J. Exp. Zool.* **148**, 185-203.
- Yoon, S.-Y. and Fissore, R. A. (2007). Release of phospholipase C zeta and [Ca²⁺]_i oscillation-inducing activity during mammalian fertilization. *Reproduction* **134**, 695-704.
- Yoshida, N. and Perry, A. C. F. (2007). Piezo-actuated mouse intracytoplasmic sperm injection (ICSI). *Nat. Protoc.* **2**, 296-304.

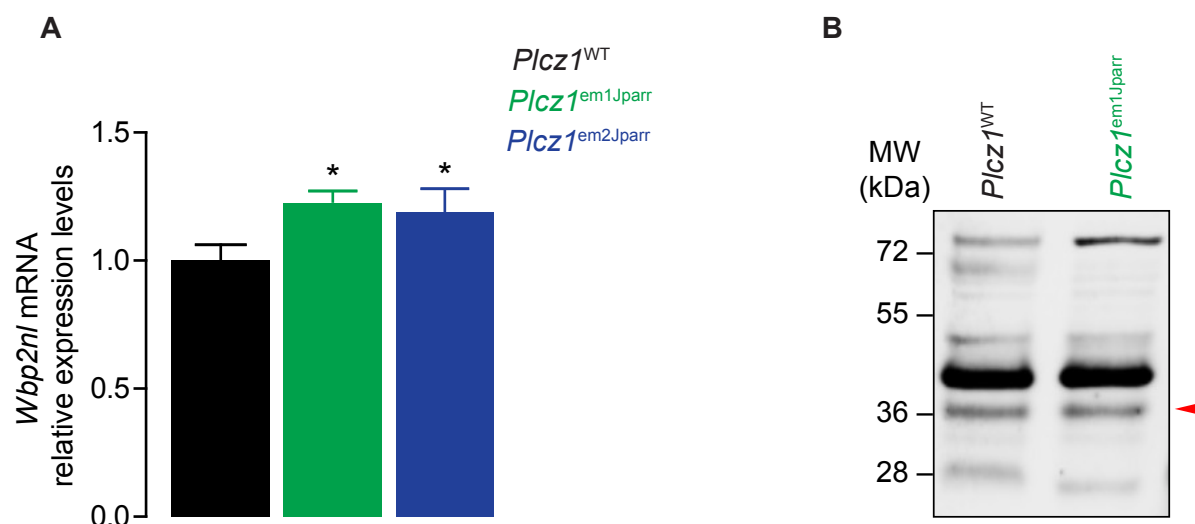


Figure S1. Expression levels of *Wbp2n*/PAWP in *Plcz1* mutant lines.

(A) Levels of *Wbp2n* mRNA in testis were determined by RT-qPCR using expression of β -actin as the reference housekeeping gene. Relative levels were determined by $\Delta\Delta$ Ct analysis and are shown as average \pm SEM of three different animals in triplicate, followed by a one-way ANOVA test.

(B) Whole sperm samples from *Plcz1*^{WT} and *Plcz1*^{em1Jparr} males were used in immunoblot analysis for PAWP (anti-PAWP antibody; ProteinTech). The immunoreactive band corresponding to the predicted size of mouse PAWP (37.5 kDa) is indicated by a red arrow.

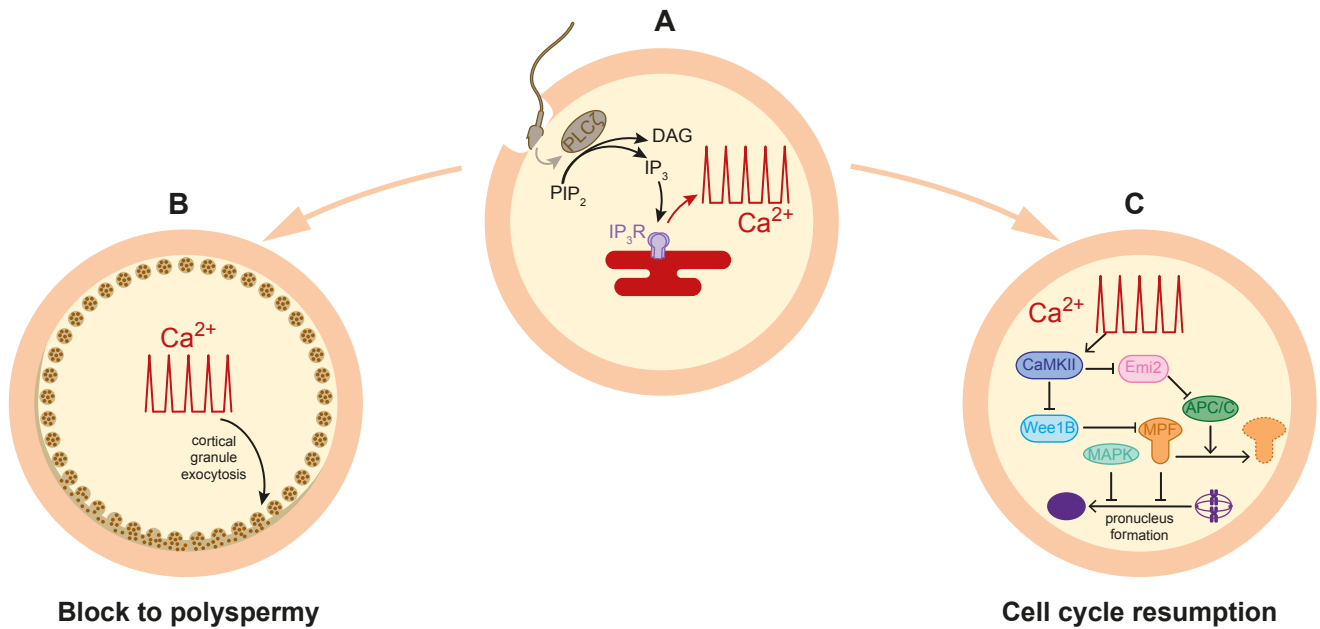


Figure S2. Role of Ca^{2+} oscillations in egg activation

(A) Delivery of PLC ζ by the sperm, induces an increase in IP₃ levels in the egg, leading to release of Ca^{2+} from the endoplasmic reticulum (via IP₃Rs) and triggering a series of cytosolic Ca^{2+} oscillations.

(B) Ca^{2+} oscillations lead to block to polyspermy, via the cortical reaction. This involves the exocytosis of the cortical granules.

(C) Ca^{2+} oscillations lead to release of the egg from metaphase II arrest. Re-initiation of the cell cycle involves the initial activation of CaMKII (calmodulin-dependent protein kinase II) leading to phosphorylation and inactivation of Emi2 (early mitotic inhibitor 2) and increased activity of APC/C (anaphase promoting complex/cyclosome), which in turn promotes degradation of MPF (M-phase promoting factor). CaMKII can also phosphorylate and inhibit Wee1B, an inhibitor of MPF. Reduced levels of MPF and MAPK (mitogen activated protein kinase) allow re-entry to anaphase and pronucleus formation.